Journal of Fluorine Chemistry 132 (2011) 459–467

Contents lists available at ScienceDirect

Journal of Fluorine Chemistry

journal homepage: www.elsevier.com/locate/fluor

Intra-cluster proton transfer in anilide–$(HF)_n$ (n = 1–4): Can the size of HF cluster influence the $N^-\cdots H–F \rightarrow N–H\cdots F^-$ switching

Hossein Roohi *, Reza Taghezadeh

Department of Chemistry, Faculty of Science, University of Guilan, Namjoh Streat, Rasht, Iran

ARTICLE INFO

Article history:
Received 11 January 2011
Received in revised form 28 April 2011
Accepted 28 April 2011
Available online 6 May 2011

Keywords:
Proton transfer
Anilide ion
HF cluster
Binding energy
MP2 and DFT methods

ABSTRACT

The impact of the HF cluster size on the proton-transfer switch between $N^-\cdots H–F$ and $N–H\cdots F^-$ in the anilide–$(HF)_{n=1-4}$ complexes was investigated by means of the quantum chemical methods. The change in the H-bond strength due to variation of the HF cluster size was well monitored by change in the binding energy (BE), structural parameter, electron density topology, natural charge and charge transfer. For n = 1, our results at the MP2/6-311++G(2d,2p) level show that the minimum-energy structure corresponds to the H-bonded complex $PhNH^-\cdots HF$ with excess negative charge localized on the N atom of the anilide anion. For $n > 1$, minimum energy structures correspond to $PhNH_2\cdots F^-(HF)_{1-3}$ ones, namely a solvated F^- ion. This is a case in which the relative change in the acidity of the HF is observed in the ground state as the size of cluster increases. The nature of the weak interactions in the complexes was characterized by means of atoms in molecules (AIM) and the natural bond orbital (NBO) analyses.

1. Introduction

Proton transfer is a common phenomenon in the chemical and biological sciences [1–3]. Ionic hydrogen bond (IHB) interactions are implicated in ionic crystals and clusters, ion solvation, electrolytes and acid–base chemistry. The strength of ionic hydrogen bond (IHB) ranges from 5 to 35 kcal/mol, and one of the strongest known examples is the FHF^- anion. The importance of this interaction in proton solvation, surface phenomenon, self-assembly process in the supramolecular chemistry, and biomolecular structure has also been recognized. The formation of IHB in simple H-bonded complexes involves partial proton transfer from the donor to the acceptor [4].

Aniline can operate as a Broensted base (pK_b = 4.596 in water) and also as a weak acid (pK_a = 30.6 in DMSO). In acidic media, aniline can form the anilinium cation in which N–H may also be involved in H-bonding as a proton donor, and in strongly basic media, aniline can form the anilide anion in which, negatively charged, the nitrogen atom acts as a strongly basic center. Szatyłowicz et al. have investigated H-bonded complexes of aniline with HF/F^- and anilide with HF at B3LYP/6-311+G(d,p) level [5] and the effects of H-bonding on the aromaticity of the ring in variously substituted complexes aniline/anilinium/anilide with bases and acids [6]. It is remarkable that in the gas phase HF is a weaker acid than aniline by ~5 kcal/mol [7]. The acidity of HF causes that in the case of complex with aniline the favorable structure to be $PhNH^-\cdots HF$. Thus, proton-transfer chemical reaction $PhNH_2\cdots F^- \rightarrow PhNH^-\cdots HF$ is thermodynamically favorable. However, in the case of interaction between anilide ion and HF, Szatyłowicz et al. [5] have showed that the optimization at the B3LYP/6-311+G(d,p) level leads to the collapse of the structure to the $PhNH_2\cdots F^-$ form. Thus, investigation of structure of $PhNH^-\cdots HF$ complex using the MP2 method in conjunction with the 6-31++G(d,p), 6-31++G(2d,2p) and 6-311++G(2d,2p) basis sets can be an important issue. Yet, there is an important question about the gas phase acidity of HF: Can the relative acidity of HF as a proton donor changes by the extent of solvation or can the anilide–HF system switches completely from $PhNH^-\cdots HF \rightarrow PhNH_2\cdots F^-$? How does the system this switching? To the best of our knowledge, influence of the size of HF cluster on the transfer of proton between HF and anilide anion has not been reported. In the second part of this work, we will investigate the structure of anilide–$(HF)_n$ (n = 1–4) and will give some answers to the above important questions. In third part of this work, nature of weak interactions in the complexes will be investigated by atoms in molecules (AIM) and the natural bond orbital (NBO) analyses.

2. Results and discussions

2.1. Geometries

The effect of size of HF cluster on the switch between $HN^-\cdots H–F$ and $N–H\cdots F^-$ proton transfer in anilide–$(HF)_{n=1-4}$ complexes were investigated by means of quantum chemical methods. The

* Corresponding author.
E-mail addresses: hroohi@guilan.ac.ir, hrouhi@gmail.com (H. Roohi).

0022-1139/$ – see front matter © 2011 Elsevier B.V. All rights reserved.
doi:10.1016/j.jfluchem.2011.04.018

optimized structures at the MP2/6-311++G(2d,2p) level of theory are depicted in Fig. 1. It is notable that each of the $n = 3$ and 4 complexes have two isomers. As can be seen in Fig. 1, **A–C** complexes have open structures while **D**, **E** and **F** have closed ones. Analysis of various aspects of H-bonded complexes revealed that the H-bond, H–F, N–H, *ipso*-ortho C–C and C–N bond distances and the ipso angles are strongly affected by change in the cluster size of HF.

In order to find the global minimum structure of anilide–HF complex, potential energy scan was performed at the MP2/6-311++G(2d,2p) level by fixing the N7···H9 distance and optimizing the remaining degree of freedom in each step of the energy scan using an 0.05 Å decline. Fig. 2 represents the dependence of the energy of complex on the N7···H9 distance. As can be seen, N7···H9 distance in global minimum structure of the anilide–HF complex is 1.357 Å. Thus, global minimum structure for interaction between anilide ion and HF molecule at the MP2/6-311++G(2d,2p) level corresponds to the $PhNH^{-}\cdots HF$ ion. As it was explained in Section 1, HF is a weaker acid than aniline in the gas phase. In the case of complex with anilide ion, acidity of HF causes the favorable structure to be $PhNH^{-}\cdots HF$, in agreement with the structure obtained at the MP2/6-311++G(2d,2p) level of theory. Thus, H-bonded complex $PhNH^{-}\cdots HF$ is formed without the proton transfer. It should be noted that we have also found the $PhNH^{-}\cdots HF$ structure is not a minimum-energy structure at the MP2/6-31++G(d,p), MP2/6-31++G(2d,2p), B3LYP/6-31++G(d,p), B3LYP/6-31++G(2d,2p) and B3LYP/6-311++G(2d,2p) levels of theory. In other world, favorable structure at these levels of theory is the $PhNH_2\cdots F^{-}$ as predicted by Szatyłowicz et al. Among the levels of theory used in this work, $PhNH^{-}\cdots HF$ is a global minimum only at MP2/6-311++G(2d,2p) level, in agreement with the experimental result [7]. This means that the increase in the size of valence shell orbitals strongly influence the optimized geometries of the H-bonded complexes.

For $(HF)_{n>1}$, minimum energy structures correspond to the $PhNH_2\cdots F^{-}(HF)_{1-3}$ which F^{-} ion is solvated by aniline and HF molecules. For $n > 1$, the proton is transferred from HF to anilide ion. Local minima corresponding to $PhNH^{-}\cdots(HF)_{2-4}$, namely a solvated anilide ion, were not found at all levels of calculation. Consequently, this is a case in which the relative change in the acidity of HF is observed in the ground state as the size of cluster increases. It seems that the relative stability of the ionic conjugate base is the driving force for the change in the acidity of the HF. On the other hand, base strength of anilide ion depends not only on the

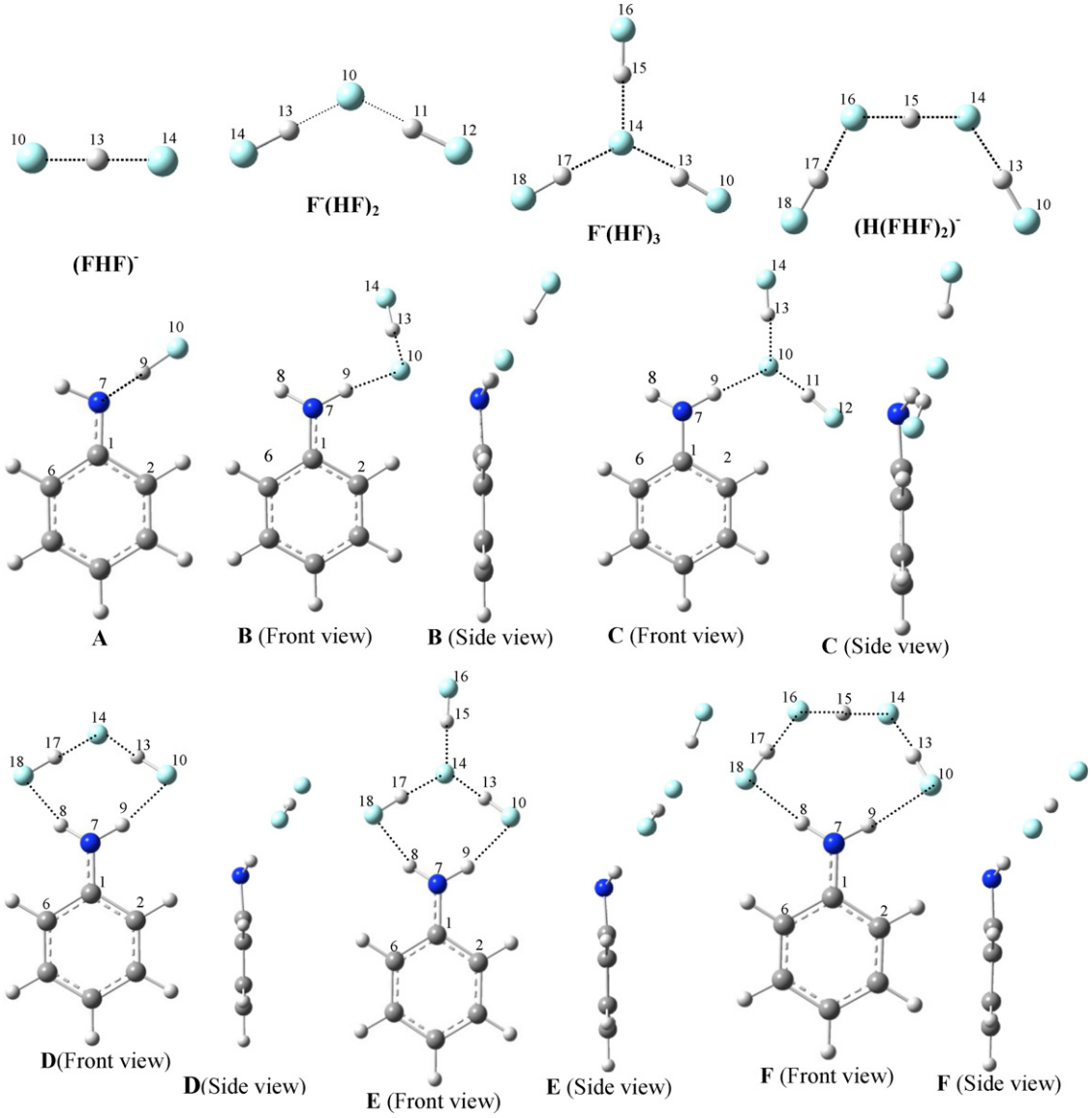

Fig. 1. The optimized structures for $F^{-}(HF)_m$ and complexes **A–F** in the gas phase.

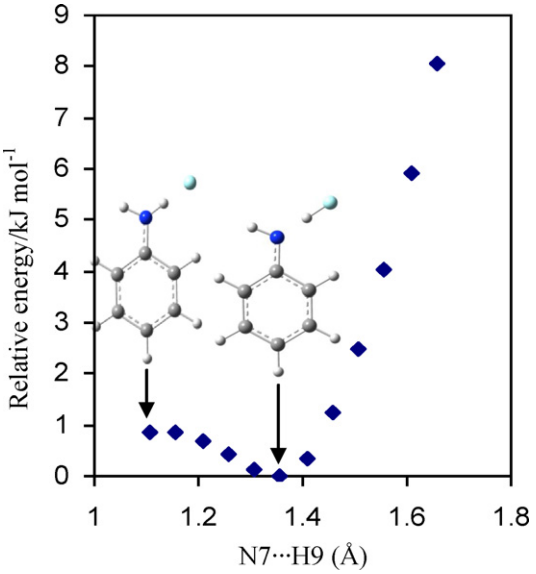

Fig. 2. Relationship between the relative energy of complex and N7···H9 distance at the MP2/6-311++G(2d,2p) level of theory.

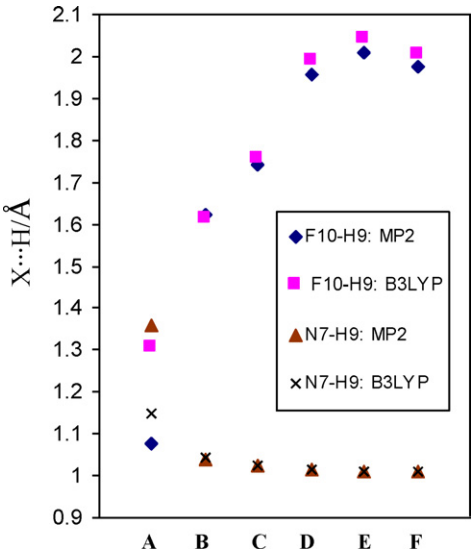

Fig. 3. Dependence of F10···H9 and N7···H9 bond distances on the size of the HF cluster.

availability of the unshared pairs for sharing with a hydrogen ion but also the environment in which it is surrounded.

The selected structural parameters for complexes **A**–**F** are given as supplementary data in Table S1. The length of N7···H9 bond at the MP2/6-311++G(2d,2p) level of theory decreases from 1.357 Å in anilide–HF (**A**) complex to 1.040, 1.025, 1.013, 1.011 and 1.011 Å in **B**–**F**, respectively. The larger distance in **A** represents the H-bonding. The average value of 1.022 Å in other complexes indicates the covalent N–H bonding which is slightly elongated by H-bonding to the F^- ion. The F10···H9 distance in complexes **A**–**F** is 1.077, 1.620, 1.743, 1.959, 2.008 and 1.975 Å at the MP2/6-311++G(2d,2p) level of theory, respectively. Although distance of N7···H9 bond in **E** and **F** is equal, but F10···H9 distance in **F** is smaller than **E**. Fig. 3 presents the dependence of F10···H9 and N7···H9 bond distances on the size of the HF cluster. As can be seen, increase in size of HF cluster is accompanied by the increase of F10···H9 bond distance and decrease of N7···H9 one. Thus, the stronger the N7···H9 bond is, the longer the F10···H9 bond is. There is a simple interpretation: increase in size of the cluster is associated with an increase in stability of F^- anion solvated by HF molecules.

Sum of bond angles around the nitrogen atom, θ, can be used to describe the shape of NH_2 group. At the MP2/6-311++G(2d,2p) level, for anilide–HF (**A**) $\theta = 359.4^\circ$ which decreases to 344.9°, 343.2°, 343.6°, 342.8° and 343.1° in complexes **B**–**F**, respectively. As the size of cluster increases, planar anilide subunit in the complex **A** is converted to the non-planar aniline one in the **B**–**F** complexes. There is a correlation between θ value and F10···H9 H-bonding distance. Correlation between θ bond angle and F10···H9 bond distance is presented in Fig. 4a. As expected, decrease in F10···H9 bond distance is associated with the increase in θ value.

The length of C–N bond, as an another measure of H-bond strength, undergoes the remarkable increase of 0.007 Å in **A**, 0.036 Å in **B**, 0.044 Å in **C**, 0.035 Å in **D**, 0.039 in **E** and 0.039 Å in **F** with respect to the free anilide (1.340 Å). Thus, an increase in size of $(HF)_n$ cluster in open structures from $n = 1$ (**A**) to $n = 3$ (**C**) is accompanied by an increase in the length of C–N bond of anilide. Besides, same trends are observed in closed structures **D** and **E** (**F**). As it has been explained in the literature [6], increase in the size of the cluster and in turn increase of the N7···H9 strength is associated by the decrease in mobility of the lone pair of nitrogen and consequently decrease in weight of the quinoid-like structure, because it becomes a partner for H-bond formation.

H-bonding leads to change in bond angles of the benzene ring in the vicinity of the H-bonding site. The C6–C1–C2 angle is 113.5° in the anilide anion that changes to 115.2°, 117.8°, 118.1°, 117.5°,

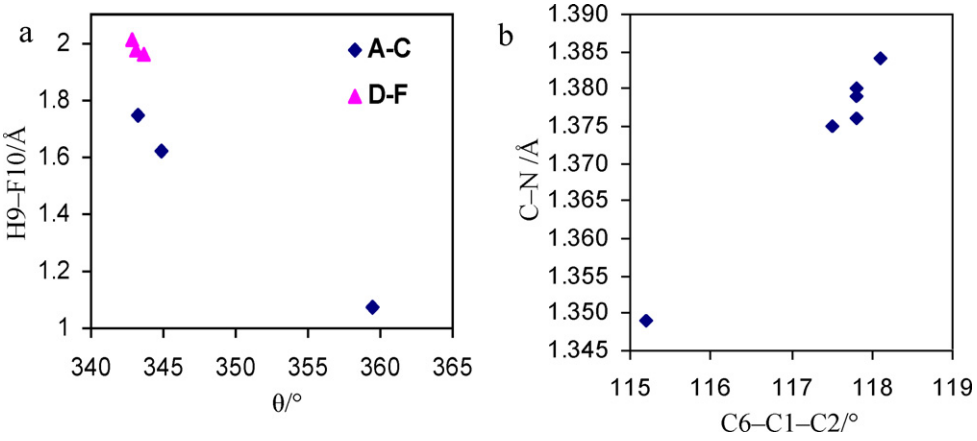

Fig. 4. (a) Correlation between H9–N–H8 bond angle and N7···H9 bond distance. (b) Correlation between C6–C1–C2 bond angle and C–N bond distance.

117.7 and 117.8° in the **A–F** complexes, respectively. Fig. 4b presents the dependence of C6–C1–C2 bond angle on the C–N bond length. As can be seen, increase in the C–N bond length is accompanied by an increase in the bond angle. In addition, C1–C2 and C1–C6 bond lengths are 1.439 and 1.442 Å in free anilide anion, respectively, which decrease upon H-bonding formation. This due to the fact the distribution of the lone pair electron of nitrogen through the H-bonding causes the decrease in the mesomeric interaction of the lone pair of nitrogen with the π-electron of the ring and consequently decrease in the C1–C2 and C1–C6 bond lengths.

Although this work has focused on the transfer of proton from HF to anilide ion, investigation of the structural parameters of superhalogen anions $F^-(HF)_m$ (m = 1–3) is also of interest. The structural parameters for $F^-(HF)_m$ at the MP2/6-311++G(2d,2p) and B3LYP/6-311++G(2d,2p) levels of theory are given in Table 1. The halogen–hydrogen bond lengths in these species are larger than that of free HF molecule. The H–F distance in the free HF molecule and FHF^- anion at the MP2/6-311++G(2d,2p) level is 0.918 and 1.142 Å, respectively. The H9–F10 and F10–H13 distances are stretched upon complex formation of **A** and **B** by 0.159 Å and 0.167 Å, respectively. In the complex **B**, terminal H–F (i.e. F14–H13) is shortened upon complexation by 0.120 Å. It is also interesting to note that the H-bond distance in the FHF^- is smaller than that of HF dimer (1.830 Å). Therefore, it would be difficult to classify FHF^- as a molecule or a complex bound by hydrogen bonds. There is a noticeable dependence of the computed F–F distance on the level of theory, as given in Table 1. This distance is 2.285 Å and 2.295 Å at the MP2/6-311++G(2d,2p) and B3LYP/6-311++G(2d,2p) levels of theory, respectively. These values are in agreement with the experimental F–F distance of 2.278 Å obtained from microwave spectroscopy [8].

The most stable structure of $F^-(HF)_2$ has the V shape with C2v-symmetry. (See Fig. 1). Upon formation of $F^-(HF)_2$, H–F covalent bond calculated at the MP2/6-311++G(2d,2p) level of theory is elongated by 0.080 Å with respect to the free HF (0.918 Å). Besides, H···F distance increases from 1.142 Å in F-HF to 1.365 Å in $F^-(HF)_2$. The HF bonds involved in interaction with the aniline are elongated upon complex formation of **C** and **D**. It should be noted that in the complexes **C** and **D**, NH_2 is interacting with the F^- anion and two HF bonds, respectively.

The superhalogen $F^-(HF)_3$ has two configurations with symmetry of C_{2v} and D_{3h} so that D_{3h} structure is more stable than C_{2v} one. In C_{2v}-symmetry, middle H atom is interacting with two FHF fragments so that it is indeed playing the role of a central atom in the superhalogen anion. The shorter bonds are formed by the terminal fluorine atoms. The covalent H–F bonds in C_{2v}-symmetry are longer and F–H···F H-bond distances are shorter than those found in D_{3h}-symmetry. The two middle F–H–F distances in C_{2v}-symmetry (1.141 Å) are closer to those of the free F^-HF (1.142 Å) and are much smaller than those found in D_{3h}-symmetry (1.468 Å). The H···F distance in D_{3h}-symmetry (1.468 Å) of $F^-(HF)_3$ is longer than that obtained in $F^-(HF)_2$ (1.365 Å), indicating that the addition of a HF molecule causes the weakening of the H-bond.

The H-bond distances in $F^-(HF)_3$ change upon complex formation. Obviously, the corresponding HB strength also changes upon complexation, depending on the shape of HF cluster. As can be seen in Table S1 and Table 1, two H13···F14 and H17···F14 distances in the $F^-(HF)_3$ decrease by 0.046 Å and H···F bond distance in which is not involved in interaction (F14···H15) increases by 0.023 Å upon complexation of aniline-$F^-(HF)_3$ (**E**). The middle F–H–F distances in F (1.140 Å) are closer to those in free $F^-(HF)_3$ with C_{2v}-symmetry (1.141 Å) while F–H···F distances decrease from 1.464 Å in free ion to 1.421 Å in complex **F**. Thus, H···F H-bonds are strengthened upon formation of **F**. It should be noted that the formation of **F** complex is accompanied by shortening of all H–F and F–F distances. Thus, all H–F contacts are strengthened upon formation of **F** complex.

2.2. Binding energies.

The electronic binding energies (BEs) of the analyzed complexes together with changes in related thermodynamic functions calculated at the various levels of theory are given as supplementary data in Table S2. Changes in thermodynamic functions upon formation of complexes at MP2/6-311++G(2d,2p) level of theory are listed in Table 2. The electronic BE of the complexes was calculated by the following equations:

$$BE = E_{complex} - (E_{HF} + E_{anilide}) \quad \text{for complex } \mathbf{A}$$

$$BE = E_{complex} - (E_{F^-}(HF)_m + E_{aniline}) \quad \text{for complexes } \mathbf{B}\text{–}\mathbf{F}$$

The changes in strength of anilide–HF and aniline–$F^-(HF)_m$ H-bonds due to variation of HF cluster size were well monitored by

Table 1
The optimized geometrical parameters (distances in Å and angles in°) for $F^-(HF)_m$ at the two levels of theory.

	FHF^-	$F^-(HF)_2$	$F^-(HF)_3$	$(H(FHF)_2)^-$
MP2/6-311++G(2d,2p)				
F10–H13	1.142 (0.918)[a]	1.365	0.967	0.975
H13–F14	1.142	0.998	1.468	1.464
F14–H15			1.468	1.141
H15–F16			0.967	1.141
F14(16)–H17			1.468	1.464
H17–F18			0.967	0.975
F10···F14	2.285	2.363	2.435	2.437
F14(16)···F18			2.435	2.437
F14···F16			2.435	2.282
B3LYP/6-311++G(2d,2p)				
F10–H9				
F10–H13	1.148	1.352	0.976	0.973
H13–F14	1.148	1.009	1.455	1.464
F14–H15			1.455	1.140
H15–F16			0.976	1.140
F14(16)–H17			1.455	1.464
H17–F18			0.976	0.973
F10···F14	2.295	2.361	2.430	2.435
F14(16)···F18			2.430	2.435
F14···F16			2.430	2.279

[a] For free H–F.

Table 2
Changes in thermodynamic functions (kJ/mol with the exception of ΔS) upon complex formation at the MP2/6-311++G(2d,2p) level of theory.

Complex	ΔE_{elec}(BE)	ΔE_0[a]	ΔE[b]	ΔH	ΔG	ΔS/J
A	−131.5	−125.0	−121.4	−123.9	−82.1	−140.4
B	−83.0	−79.4	−71.9	−74.4	−47.2	−91.3
C	−68.1	−64.3	−55.4	−57.9	−25.6	−108.6
D	−70.0	−67.2	−60.6	−63.1	−23.1	−134.2
E	−57.6	−54.6	−47.0	−49.5	−11.2	−128.6
F	−61.4	−57.7	−47.8	−50.3	−18.3	−107.3

[a] $\Delta E_0 = \Delta E_{elec} + \Delta ZPE$.
[b] $\Delta E = \Delta E_0 + \Delta E_{therm}$.

changes in the defined electronic binding energies. The BE energy at the MP2/6-311++G(2d,2p) level of theory for complex **A** according to the reaction *anilide ion* + HF → *anilide*–(HF) is −131.5 kJ/mol and those of complexes **B**–**F** according to the reaction *aniline* + $F^-(HF)_{1,2,3}$ → *aniline*–$F^-(HF)_{1,2,3}$ are −84.4, −67.6, −69.5, −57.6 and −61.4 kJ/mol, respectively. This situation is observed at all levels of theory. Dissociation energy D_e (–BE) of complexes decreases as the number of the HF in the $F^-(HF)_m$ cluster increases.

There is a correlation between D_e (–BE) of complexes and the corresponding H-bond distances. This relationship is shown in Fig. 5a. As can be seen, D_e decreases as the corresponding H-bond distance increases. Thus, as the size of $F^-(HF)_m$ cluster in complexes increases, F^- anion is better solvated by HF molecules and the $F^-(HF)_m$ cluster tends to be separated from aniline fragment. These results confirm that the base strength of an ion depends not only on the availability of the unshared pairs for sharing with a hydrogen ion but also the environment in which it is surrounded. Fig. 5b shows the schematic representation of the absolute value of electronic BE for **A**–**F** complexes at the various levels of theory.

The electronic BEs are sensitive to methods and basis sets used in the calculations. Looking at Table S2, we find that the B3LYP BEs are greater than the MP2 ones using the same basis set. In addition, BE decreases as the size of basis set increases from 6-31++G(d,p) to 6-311++G(2d,2p). Besides, although zero-point vibrational energy (ZPVE) correction has a significant effect on the BE of complexes, but inclusion of ZPVE does not changes the order of BE of complexes. From Table 2 and Table S2, it can be concluded that the complexation at all levels of theory is accompanied by a decrease in Gibbs free energy, enthalpy and entropy (i.e. $\Delta G < 0$, $\Delta H < 0$ and $\Delta S < 0$). Although at room temperature $\Delta S < 0$, ΔH is sufficiently negative to outweigh the contribution of the entropy decrease.

Table 3
Vibrational frequencies (cm^{-1}) at the B3LYP/6-311++G(2d,2p) level of theory.

	ν_1	ν_2	ν_3
HF	4165.7		
F^-HF	619.8[a]	1276.3[b]	1335.4[c]
$F^-(HF)2$	2650.3	2319.1	1200.9
$F^-(HF)3$	3217.2	2944.7	1066.9
$(H(FHF)_2)^-$	3130.0	3102.0	
Aniline	3663.0[d]	3570.3[e]	1664.3[f]
A	1653.8[g]		
B	3645.6[d]	2987.1[e]	1714.4[f]
C	3643.3	3304.3	1707.7
D	3565.0	3473.8	1726.8
E	3597.0	3505.2	1718.0
F	3596.0	3496.1	1721.3

[a] Symmetric stretching.
[b] Asymmetric stretching.
[c] Bending.
[d] Vibrational modes for NH_2 group.
[e] Vibrational modes for NH_2 group.
[f] Vibrational modes for NH_2 group.
[g] H–F stretching at MP2/6-311++G(2d,2p).

2.3. Vibrational frequency analysis

Geometrical changes induced by the formation of complex are accompanied by the shifts in the vibrational frequencies with respect to those of their constituents. Inspection of the vibrational frequencies shows that the complex formation results in a marked change of vibrational frequency of D–H (D denotes donor proton) bonds involved in H-bonding. The selective vibrational frequencies are given in Table 3. Since global minimum structure of the anilide–$(HF)_1$ is obtained only at the MP2/6-311++G(2d,2p) level of theory, we have reported the vibrational frequency of this complex at the mentioned level. For other complexes, we have used the B3LYP/6-311++G(2d,2p) vibrational frequencies since both MP2 and B3LYP methods reproduce very similar geometrical structures for aniline–$F^-(HF)_m$ complexes. As expected, interaction leads to increase in D–H bond distance and consequently a substantial red-shift in the fundamental D–H stretching vibrational frequency. From the analysis of frequencies, it is found that the amount of red-

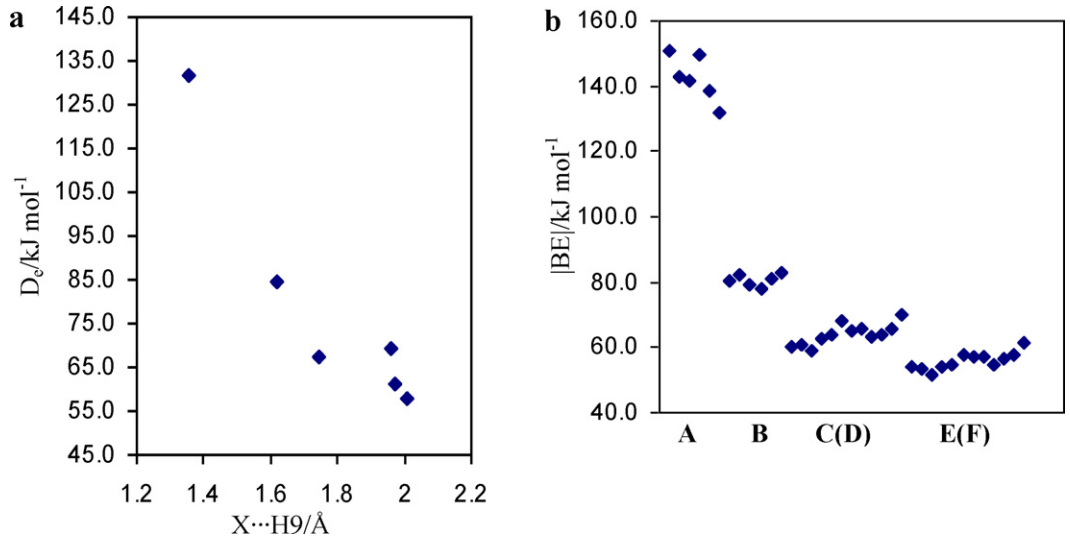

Fig. 5. (a) Correlation between dissociation energy of **A–F** complexes and X···H9 (X = N or F) bond distance. (b) Schematic representation of the absolute values of the binding energies (BEs) at the six levels of theory.

shift of H–F vibrational frequency in formation of anilide–HF is 2511.7 cm^{-1} with respect to the corresponding free HF vibrational mode at 4165.2 cm^{-1}. The red-shifts of N–H9 stretching frequencies in formation of aniline–F(HF)$_m$ (**B–F**) complexes are, respectively, 583.2, 266.0, 96.5, 65.1 and 74.2 cm^{-1} with respect to the symmetrical vibrational mode of free aniline at 3570.3 cm^{-1}. Thus, in agreement with an increase in H9···F10 distance, red-shift of N–H9 vibrational frequency decreases as the size of HF cluster increases. Our calculations also predict that the frequency of the NH_2 bending vibrational mode in the complexes **B–F** is blue-shifted by 50.1, 43.4, 62.5, 53.7 and 57.0 cm^{-1} compared to the free aniline (1664.3 cm^{-1}).

It should be interesting to compare the vibrational frequencies in free HF clusters. The symmetric stretching vibrational frequency of F^-HF at the B3LYP/6-311++G(2d,2p) level of theory is 619.8 cm^{-1} that is closer to the experimental value of 583 cm^{-1} [8]. The asymmetric and bending vibrational frequencies are 1276.3 and 1335.4 cm^{-1}, which are comparable with the experimental values of 1286.0 and 1331.0 cm^{-1}, respectively. The vibrational frequencies increases on going from F^-HF to $F^-(HF)_2$, in good agreement with the decrease in H–F bond length. The symmetric stretching, asymmetric stretching and bending frequencies in $F^-(HF)_2$ are 2650.3, 2319.1 and 1200.9 cm^{-1}, respectively. The $F^-(HF)_3$ cluster with D_{3h}-symmetry has three greater vibrational frequencies centered at 3217.2, 2944.7 and 1066.9 cm^{-1} which correspond to the symmetric stretching, asymmetric stretching and the bending vibrational modes, respectively. As discussed previously, terminal H–F bonds are strengthened on going from $F^-(HF)_2$ cluster to $F^-(HF)_3$ one. Thus, increase in stretching vibrational frequencies is logical. Two greater vibrational frequencies are appeared at 3130.0 and 3102.4 cm^{-1} for $H(F^-HF)_2$ with C_{2v}-symmetry.

2.4. AIM analysis

The topological parameters derived from the Bader theory are often used as descriptors of H-bond strength. Topological criteria are also useful in detecting the existence of H-bond interactions [9,10]. The calculated values of electron density, $\rho(r)$, Laplacian of electron density, $\nabla^2\rho(r)$, and electronic energy density, $H(r)$, at the bond critical points (BCPs) at the MP2/6-311++G(2d,2p) level of theory are given as supplementary data in Tables S3 and S4. The molecular graphs (including the critical points and bond paths) for all of the complexes are shown in Fig. 6. Besides all of the expected BCPs, the electron density reveals the additional BCPs and ring critical points.

The electron density at H9···X (X = F and N) bond critical point gauges the strength of the intermolecular H-bond interaction,

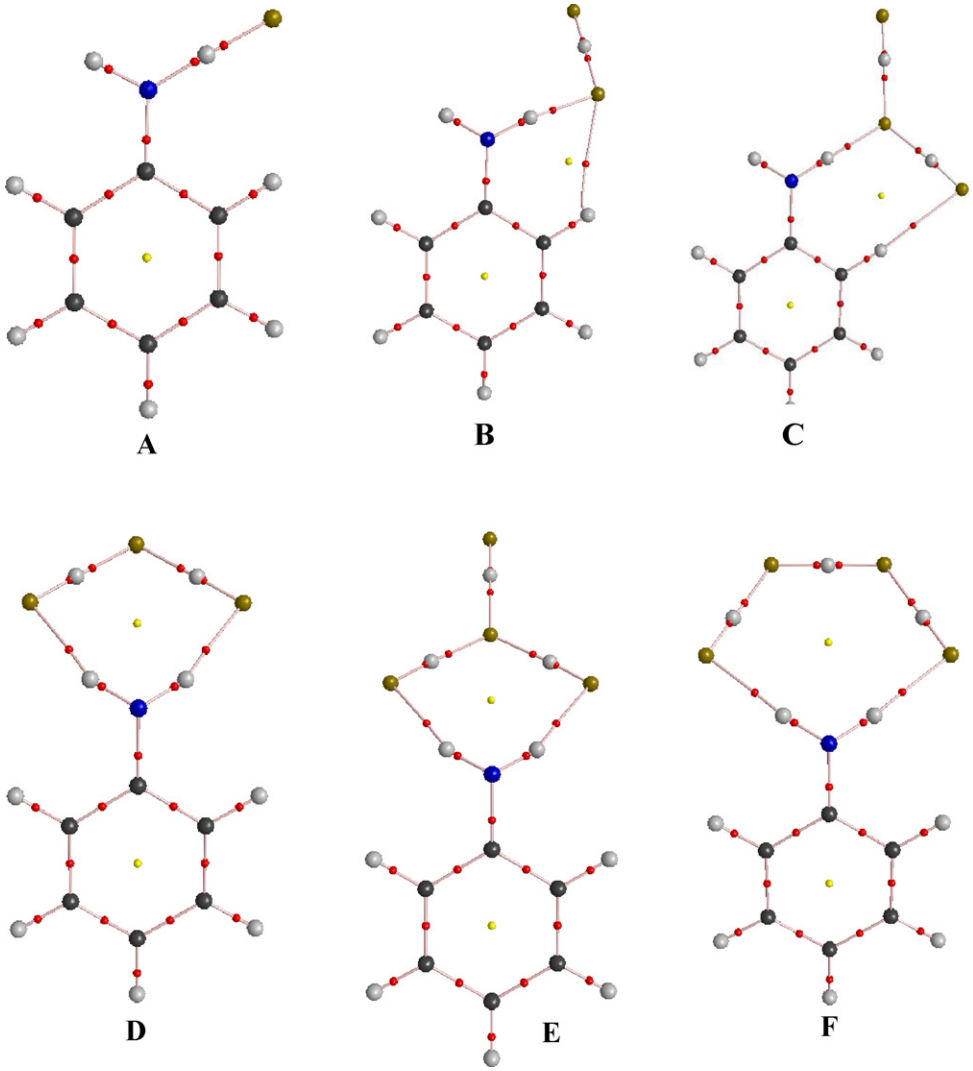

Fig. 6. Molecular graphs of the anilide–HF (**A**) and aniline–$F^-(HF)_m$ (m = 1–3) (**B–F**) complexes. Nuclei and critical points (bond and ring) are represented by big and small circles, respectively.

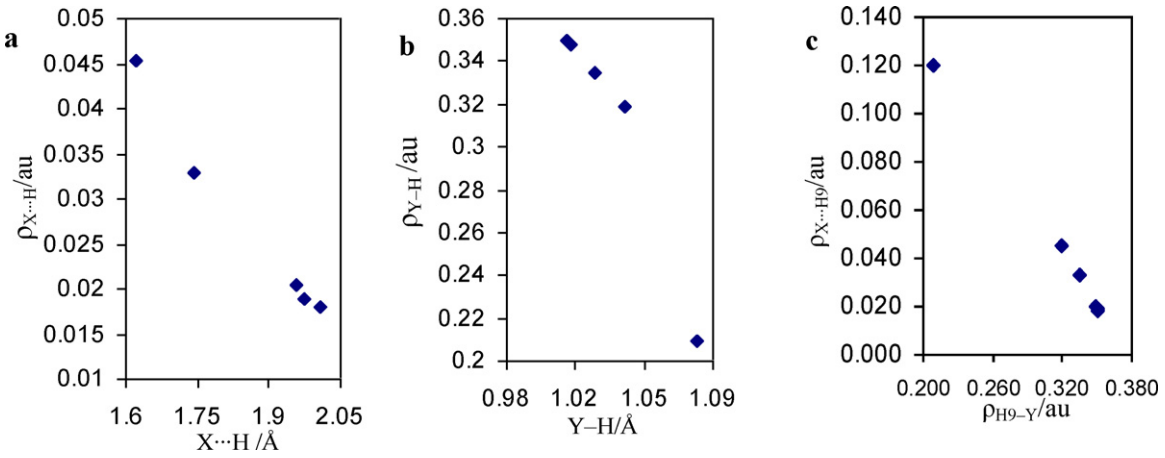

Fig. 7. (a) Correlation between $\rho(r)$ at the N···H9 and F···H9 (defined as the X···H) HBCPs and the corresponding H-bond distances (b) Correlation between $\rho(r)$ at the F–H9 and N–H9 (defined as the Y–H) BCPs and the corresponding bond lengths. (c) Correlation between the $\rho_{X\cdots H9}$ and ρ_{H9-Y} in the **A–F** complexes.

which are manifested by distance between H9 and X. Correlation between $\rho(r)$ at the X···H9 and Y–H9 BCPs and the corresponding H-bond distances are given in Fig. 7 a and b, respectively. Fig. 7c shows the dependence between the $\rho_{X\cdots H9}$ and ρ_{H9-Y}. As can be seen, increase in $\rho(r)$ at H9–Y BCP is accompanied by a decrease in $\rho(r)$ at X···H9 BCP. Our results show that the $H(r)$ and $\bigtriangledown^2\rho(r)$ properties at N7···H9 BCP of the complex **A** have negative values of −0.1036 au and −0.0884 au, indicating the covalent nature of the H-bonding. The H9···F10 interaction in the complex **B** is characterized by positive $\bigtriangledown^2\rho(r)$ (0.1702 au) and negative $H(r)$ (−0.0019 au) values. This indicates the partially covalent nature of H9···F10 interaction. However, analysis of the electron density properties in the **C**–**F** complexes shows that the both $H(r)$ and $\bigtriangledown^2\rho(r)$ properties at NH···F BCPs have positive values, indicating electrostatic nature of the H-bonding.

As can be seen in Tables S3 and S4, electron density at C–N BCP decreases upon complex formation of **A** by 0.0086 au. The $N^-\cdots HF$ H-bonding in complex **A** decreases the mobility of the lone pair at the nitrogen atom and decreases mesomeric effect. In contrast, electron density at C–N BCP of **B**–**F** complexes increases compared to the aniline (0.3042 au). Therefore, it is expected that the mobility of the lone pair at the nitrogen atom and in turn mesomeric effect increases. Decrease in the strength of the $NH_2\cdots F$ interaction on going from **B** to **F** is accompanied by a decrease in mobility of the lone pair, leading to decrease in $\rho(r)$ at C–N BCP. As can be seen in Table S3, in contrast to the C–N bond, $\rho(r)$ of ipso C1–C2 bond increases when the strength of $NH\cdots F^-$ interaction decreases.

It is interesting to note the changes in the electron density properties of HF clusters upon complex formation. As expected, cluster formation causes a marked decrease of electron density of the H–F bond. As can be seen in Table S4, $\rho(r)$ and $H(r)$ values at the H–F BCP of all HF clusters is smaller than those of free HF molecule. The values of $\rho(r)$ and $H(r)$ at H–F BCP of free HF molecule are 0.3807 au and −0.9743 au and those of FHF^- anion are 0.1678 au and −0.2510 au, respectively, indicating that the strength of H–F bond and in turn its covalent nature strongly decreases upon formation of FHF^-. All of the H13···F14 H-bonds in $F^-(HF)_m$ clusters have positive $\bigtriangledown^2\rho(r)$ and negative $H(r)$ values. This indicates that these H-bonds are covalent in nature. The $\rho(r)$ and $H(r)$ values at H13···F14 H-bonds in $F^-(HF)_m$ clusters are smaller than F10–H13 ones.

The $\rho(r)$ and $\bigtriangledown^2\rho(r)$ values at H–F BCP decrease upon complex formation of **A** from 0.3807 au and −1.5228 au to 0.2092 au and −1.1512 au, respectively. The electron density at BCP of H–F bond involved in interaction decreases from 0.1678 au in FHF^- anion to 0.0996 au in complex **B**. The increase in size of HF cluster causes a decrease in $\rho(r)$ of H···F BCP from 0.1678 au in F^-HF to 0.0830 au in $F^-(HF)_2$. The $\rho(r)$ at H···F BCP decreases from 0.0830 au in $F^-(HF)_2$ to 0.0676 au in complex **C**. The $\rho(r)$ at the two terminal H–F BCPs of $F^-(HF)_2$ is 0.2703 au that increases to 0.2945 au in complex **C**. Therefore, terminal H–F bonds are strengthened upon complex formation. The formation of **D** complex causes the $\rho(r)$ at the H13–F10 BCP decreases and at the H13···F14 BCP increases. Consequently, H13–F10 bond of $F^-(HF)_2$ involved in interaction with the aniline is elongated upon formation of **D** complex.

The increase in size of cluster from $F^-(HF)_2$ to $F^-(HF)_3$ causes a decrease in the $\rho(r)$ of the H13···F14 BCP and an increase in the $\rho(r)$ of the H13–F10. The electron densities at both H13···F14 and H17···F14 BCPs increase and that of the H15···F14 BCP decreases upon complexation of the aniline–$F^-(HF)_3$ (**E**), in agreement with the changes observed in H-bond distances. The values of electron density at all H···F BCPs of **F** complex are greater than the corresponding free $(H(FHF)_2)^-$, indicating that all of the HF contacts are strengthened upon complexation.

There is a good correlation between $\rho(r)$ at the H-bond critical points of mentioned compounds (complexes and free clusters) and the corresponding bond distances. Fig. 8 shows this correlation. As can be seen in this figure, increase in the H-bond distance is accompanied by the decrease in electron density of the corre-

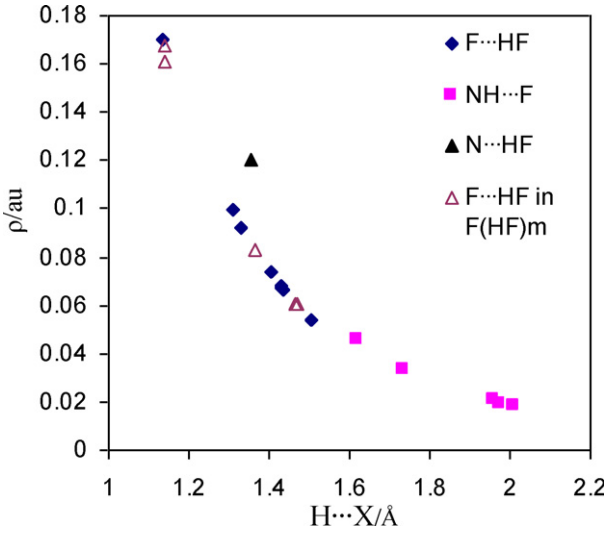

Fig. 8. Correlation between $\rho(r)$ at the H-bond critical points and the corresponding H···X (X = F or N) bond distances. $F(HF)_m$ means F···HF H-bonds in isolated $F^-(HF)_m$.

sponding H-bond critical point. AIM data show that the N···HF H-bond in complex **A** has covalent nature. The unusual behavior of the N···HF H-bond can be attributed to the different nature of this bond with respect to the other ones.

2.5. NBO analysis

A better understanding of the molecular interactions in the complexes is provided by NBO analysis. The formation of the hydrogen bond implies that the certain amount of the electronic charge is transferred from the proton acceptor to the proton donor molecule [11,12]. For several typical H-bonded systems, it has been demonstrated that the charge is transferred from the lone pairs of the proton acceptor to the anti-bonding orbitals of the proton donor [13]. The results of NBO analysis including charge transfer (CT), natural charge and occupancy of NBOs at the MP2/6-311++G(2d,2p) level of theory are given as supplementary data in Table S5.

The observed charge transfer amounts to a sum of the atomic charges of the proton donor subunit. The results show that the charge transfer takes place from the proton acceptor subunit to proton donor one. The value of charge transfer from anilide anion to HF in the anilide-HF complex (**A**) is 0.2099 au. In the case of **C–F** complexes, as the size of HF cluster increases, transfer of charge from $F^-(HF)_m$ fragment to aniline decreases in agreement with an increase in NH···F H-bond distances. The values of the charge transfer are 0.0677 au in aniline–F^-(HF) (**B**), 0.0903 in aniline–$F^-(HF)_2$ (**C**), 0.0357 au in aniline–$F^-(HF)_2$ (**D**), 0.0274 au in aniline–$F^-(HF)_3$ (**E**) and 0.0308 au in aniline–$F^-(HF)_3$ (**F**) complexes. Increase in size of HF cluster can influence the electron density of atoms involved in interactions. In the complex **A**, N atom is a proton acceptor while it is a proton donor in complexes **B–F**. The negative charge of N atom in free anilide ion is −0.8851 which decreases to −0.8842 in complex **A** whereas that of free aniline is −0.7988 au that increases to −0.8232, −0.8193, −0.8191, −0.8177 and −0.8219 au in complexes **B–F**, respectively. For aniline–$F^-(HF)_m$ complexes, increase in size of $F^-(HF)_m$ clusters is accompanied by a decrease in electronic charge on the nitrogen atom, with the exception of that found in complex **F**. The weaker interaction between aniline and $F^-(HF)_m$ clusters is, the lesser is the electron density at the N atom. As expected, upon increase in size of HF cluster, flow of the electron density from the lone electron pairs of the proton acceptor F to the σ^*(N–H) decreases that causes a smaller negative charge on the proton donor (N atom). This causes a strengthening of the N–H bond, its shortening, and an increasing of the N–H stretching vibrational mode.

The positive charge of H atom in free HF is 0.5429 au which decreases to 0.4959 au in anilide–HF complex. This situation is reverse for complexes **B–F**. The bridging hydrogen, H9, in the free aniline has positive charge of 0.3646 au that increases to 0.4424 au, 0.4329 au, 0.4067 au, 0.4016 au and 0.4023 au in complexes **B–F**, respectively. Change in electron density of atoms involved in H-bond interaction in complexes **B–F** is in agreement and those of found in complex **A** is in disagreement to the Koch–Popelier criteria [9,10].

The occupancy of the lone pair of nitrogen atom in the free anilide ion is 1.9629 au that decreases to 1.7890 au in the anilide–HF (**A**). Besides, occupancy of the lone pair of nitrogen atom in free aniline is 1.9051 au that decreases to 1.8469 au, 1.8650 au, 1.8486 au, 1.8586 au and 1.8572 au in **B–F** complexes, respectively. As can be seen, due to decrease in the strength of the H-bond interaction between aniline and $F^-(HF)_m$ clusters, occupancy of the lone pair of the nitrogen atom increases as the size of cluster increases. Due to the presence of the multiple H-bonded interactions, anomalous trend of these occupancies is observed.

3. Conclusions

Influence of size of HF cluster on the transfer of proton between HF and anilide anion has been investigated at the various levels of theory. In agreement with the experimental results, our results at MP2/6-311++G(2d,2p) level show that the $PhNH^-$ with a single HF forms H-bonded complex $PhNH^-\cdots HF$ without proton transfer. For $n > 1$, the proton is transferred from HF to anilide ion. Thus, minimum energy structures for $(HF)_{n>1}$ correspond to $PhNH_2\cdots F^-(HF)_{1-3}$ ones which F^- ion in them is solvated by aniline and HF molecules. It seems that the relative stability of the ionic conjugate base is the driving force for the change in acidity of the HF. Increase in size of HF cluster is accompanied with the increase in F10···H9 bond distance and decrease in N7···H9 one. Dissociation energy of complexes according to *aniline*-$F(HF)_{1,2,3} \rightarrow$ *aniline* + $F(HF)_{1,2,3}$ decreases as the number of HF in $F^-(HF)_m$ cluster increases. Thus, as the size of $F^-(HF)_m$ cluster in complexes increases, F^- anion is better solvated by HF molecules and the $F^-(HF)_m$ cluster tends to be separated from aniline fragment. In agreement with an increase in H9···F10 distance, red-shift of N7–H9 vibrational frequency decreases as the size of HF cluster increases. Our results show that N7···H9 H-bond in **A** complex has covalent nature. In addition, analysis of the electron density property shows that the values of the $H(r)$ and $\nabla^2\rho(r)$ at the H9···F10 BCP of the **B** complex are negative and positive, respectively, indicating the partially covalent nature of this H-bond. The nature of H9···F10 H-bonds in complexes **C–F** is electrostatic. The value of charge transfer from anilide ion to HF in anilide–HF complex is 0.2099 au. In the case of aniline–$F^-(HF)_m$ complexes, as the size of HF cluster increases, transfer of charge from $F^-(HF)_m$ to aniline decreases in agreement with an increase in NH···F H-bond distance.

4. Computational details

The geometries of all complexes (**A–F**) formed from interaction between anilide ion and HF clusters were optimized using the B3LYP [14] and MP2 [15] methods in conjunction with the 6-31++G(d,p), 6-31++G(2d,2p) and 6-311++G(2d,2p) basis sets [16]. The vibrational frequencies for complex **A** were calculated at MP2/6-311++G(2d,2p level of theory and for other complexes using B3LYP method in conjunction with the 6-31++G(d,p), 6-31++G(2d,2p) and 6-311++G(2d,2p) basis sets. The calculated vibrational frequencies have been used to characterize the stationary points and the calculation of zero-point vibrational (ZPV) and thermal energies. All **A–F** and $F^-(HF)_m$ structures correspond to the energy minima since no imaginary frequencies were found, with the exception of $(H(FHF)_2)^-$ anion with an imaginary frequencies of 24i cm^{-1} at B3LYP/6-311++G(2d,2p) level of theory. For complexes **B–F**, MP2 electronic energies were corrected by ZPV and thermal energies obtained by B3LYP method. All calculations were performed using the Gaussian 98 program package [17]. Topological properties of the electron density were calculated at MP2/6-311++G(2d,2p) level of theory by the AIM2000 program package [18]. The nature of three types of H-bonding interactions (N···HF, NH···F and F···HF) was characterized by means of atoms in molecules (AIM) [19] analysis. The NBO analysis [20] was carried out on the MP2/6-311++G(2d,2p) wave function using the version 3.1 of the NBO package [21] included in the Gaussian 98 program package.

Appendix A. Supplementary data

Supplementary data associated with this article can be found, in the online version, at doi:10.1016/j.jfluchem.2011.04.018.

References

[1] Y. Podolyan, L. Gorb, J. Leszczynski, J. Phys. Chem. A (12103) (2002) 12103–12109.
[2] X. Hu, H. Li, W. Liang, S. Han, J. Phys. Chem. B 108 (2004) 12999–13007.
[3] D.S. Ahn, S. Lee, B. Kim, Chem. Phys. Lett. 390 (2004) 384–388.
[4] M. Meot-Ner (Mautner), Chem. Rev. 105 (2005) 213–284, and references cited therein.
[5] H. Szatyłowicz, T.M. Krygowski, J.J. Panek, A. Jezierska, J. Phys. Chem. A 112 (2008) 9895–9905.
[6] H. Szatyłowicz, T.M. Krygowski, J.E. Zachara-Horeglad, J. Chem. Inf. Model 47 (2007) 875–886.
[7] J.W. Larson, T.B. McMahon, J. Am. Chem. Soc. 105 (1983) 2944–2950.
[8] K. Kawaguchi, E. Hirota, J. Chem. Phys. 87 (1987) 6838–6841.
[9] U. Koch, P.L.A. Popelier, J. Phys. Chem. 99 (1995) 9747–9754.
[10] P.L.A. Popelier, J. Phys. Chem. A 102 (1998) 1873–1878.
[11] P. Hobza, Z. Havlas, Chem. Rev 100 (2000) 4253–4264, and references cited therein.
[12] P. Hobza, V. Spirko, H.L. Selzle, E.W. Schlag, J. Phys. Chem. A 102 (1998) 2501–2504.
[13] A.E. Reed, L.A. Curtiss, F. Weinhold, Chem. Rev. 88 (1988) 899–926.
[14] (a) C. Lee, W. Yang, R.G. Parr, Phys. Rev. B 37 (1988) 785–789;
(b) A.D. Becke, J. Phys. Chem. 98 (1993) 1372–1377;
(c) A.D. Becke, J. Chem. Phys. 98 (1993) 5648–5652;
(d) P.J. Stephens, F.J. Devlin, C.F. Chabalowski, M.J. Frisch, J. Phys. Chem. 98 (1994) 11623–11627.
[15] (a) C. Moller, M.S. Plesset, Phys. Rev. 46 (1934) 618–622;
(b) R. Krishnan, J.A. Pople, Int. J. Quantum Chem. 14 (1978) 91–100.
[16] C.J. Cramer, Essentials of Computational Chemistry, 2nd ed., John Wiley & Sons, 2004, Chapter 6.
[17] M.J. Frisch, et al., Gaussian 98, Revision A.5, Gaussian, Inc., Pittsburgh, PA, 1998.
[18] F. Biegler-König, J. Schönbohm, D. Bayles, J. Comp. Chem. 22 (2001) 545–559.
[19] R.W.F. Bader, Atoms in Molecules—A Quantum Theory, Oxford University Press, Oxford, 1990.
[20] (a) J.E. Carpenter, F. Weinhold, J. Mol. Struct. (Theochem.) 169 (1988) 41–62;
(b) A.E. Reed, R.B. Weinstock, F. Weinhold, J. Chem. Phys. 83 (1985) 735–746.
[21] D.E. Glendening, A.E. Reed, J.E. Carpenter, F. Weinhold, NBO, Version 3.1